Supplementary material

S1. Remote sensing data source selection

In this study, we choose MODIS data instead of other satellites with higher spatial resolution (e.g. Landsat or Sentinel-2) because MODIS has several advantages in terms of data availability and quality (e.g. more years of data and cloud-free image every 16-days). Since the MODIS sensor provides a daily image of the Earth, such high frequency (1 per day) increases the probability of finding a cloud-free image every 16-days. MODIS provides the best composite value every 16 days (i.e. chooses the best available pixel value from all the acquisitions from the 16 day period), applying an algorithm that selects the image atmospherically corrected bi-directional surface reflectances and select the image with lowest cloud presence, the lowest view angle, and the highest EVI value. Although Landsat has a lower pixel size, their images have a lower frequency (i.e., 1 image every 16 days). Thus, the fixed acquisition schedule makes it less probable to acquire good-quality imagery for a particular place periodically (especially if clouds occur frequently over the area of interest, e.g. winter dates).

Landsat product with the largest time series is Landsat 7 (1999-actually) however, on May 31, 2003, the satellite's scan-line corrector failed. The scan-line corrector is a device on the satellite that keeps the scan lines parallel to each other. Without the Scan Line Corrector (SLC), the scan lines are mis-aligned and there are wedge-shaped data gaps in the images. Providers offer different procedures for filling-in the data gaps, but each amounts to using data from good images prior to 2003 to do so. Obviously the further one gets from 2003, the less valid this approach will be. Therefore, since 2003 SLC failure of Landsat 7, Landsat 8 is the only fully operational Landsat satellite in orbita, but covers a shorter time series than MODIS (Landsat8 covers from 2013 to actually, while MODIS covers from 2001 to actually).

Other satellites have also been considered for their use, as Sentinel-2, which also has a higher spatial resolution but the time series is still too short for our study (2015-present). Therefore, the period of Sentinel-2 data is not covered by FLUXNET data, i.e. Sentinel-2 starts taking data in 2015 and the available FLUXNET database goes up to this year.

S2. EC-EFT Discriminant Analysis

During the comparison of the performance of PFTs and EFTs to discriminate the seasonal dynamics of NEE, we took into account the unbalanced sample size due to the different number of classes of EFTs (20) and PFTs (7) represented by FLUXNET2015 and the different number of EC sites per PFT class (which ranged between 3 and 31). To do this we performed the following steps:

First, we calculated all possible combinations (C) without repetitions between the 18 EFT and the 7 PFT classes (C(18,7) = 31834). Second, we discarded all combinations that had different numbers of EC sites in the EFT and PFT classes being combined. Third, for each combination, we applied discriminant analysis to assess how well the EFT classification and the PFT classification performed to discriminate the seasonal dynamics of NEE. For each discriminant analysis, we obtained five metrics of performance (Table S2). Fourth, to assess whether there existed significant differences in the performance metrics between EFTs and PFTs, we applied the Wilcoxon non-parametric test. For each combination of the number of classes and the number of EC sites, there was a different number of discriminant analyses in the EFT subset and in the PFT subset (Table S1). To account for such an unbalanced design during the Wilcoxon test, we fixed the sample size to the smaller subset (either from the EFT or the PFT classification) and randomly bootstrapped the performance metrics from the bigger one. Fifth, we calculated the mean and standard deviation of each metric obtained by the EFTs and PFTs classifications, the average p-value, and the percentage of times that we obtained significant differences (p-value <0.05) between EFTs and PFTs.

To assess whether different satellite-derived EFT classes correspond to different NEE dynamics and whether sites under the same EFT exhibit similar NEE dynamics, we applied discriminant analysis. We selected the EFT of the MODIS pixel where each EC site was located and its corresponding interannual average of the seasonal cycle of NEE for the available years. EC sites' fluxes were regarded as the ground truth against which the satellite data were compared to calculate five performance metrics: Kappa, Accuracy, Precision, Recall, and F1 score (Table S2).

Table S1. Number of discriminant analysis (i.e. combinations) for each number of classes and number of EC sites in the EFT and in the PFT subsets.

		n classes EFTs						n classes PFTs					
		2	**3**	**4**	**5**	**6**	**7**	**2**	**3**	**4**	**5**	**6**	**7**
n EC sites	**3**	32						6					
	4	38	56					3	3				
	5	24	112					2	6				
	6	26	160	392				5	2	3			
	7	12	160	536				3	7	2			
	8		160	585	1078				9	3	1		
	9	10	126	592				1	3	9			
	10		96	520	1640				2	7	3		
	11	4	82	464	1668			4	3	2	5		
	12	1	60	373	1655	3504		6	21	6	2	1	
	13		50	320	1466	3868			2	3	3	1	
	14		28	238	1312				6	61	6		
	15		27	196	1112	3676			51	2	1	3	
	16		12	136	922	3396			6	41	6	2	
	17		8	100	746		7252		9	72	4		1
	18		2	54	590	2597			2	4	6	2	
	19			28	428					81	21		
	20			12	267	1817				11	16	61	
	21			4	160	1332				5	7	1	
	22			1	78	945	4153			4	21	4	2
	23				36	580	3308				13	91	2
	24				10	337					5	7	
	25				4	154	1610				12	4	7
	26					70	958					6	5
	27					20						8	
	28					6	232					4	4
	29						90						2
	30						25						3
	31						4						7

Table S2. Contingency table (in %) of EFTs and PFTs. The numbers show the percentage of EFTs classified in each PFT. EFTs are coded as follows: capital letters correspond to the EVI annual mean (EVI_mean) level, ranging from A to D for low to high productivity. Small letters show the seasonal standard deviation (EVI_SD), ranging from a to d for high to low seasonality of carbon gains. The numbers indicate the season when the maximum EVI took place (DMAX): (1) spring, (2) summer, (3) autumn, (4) winter.

%	Cropland	Deciduous broadleaf trees	Evergreen needleleaf trees	Grassland	Mixed trees	Shrubland	Wetland
Aa1				29	12		
Ab2			10				
Ac1			20				
Ac2			10				
Ad1						67	
Ad4					12	33	
Ba1	27						100
Bc1			20				
Bd1	13				25		
Bd2			10		13		
Ca1	7						
Cb1	33						
Cc1	7		10		13		
Cd1	7				25		
Cd3			10				
Da1		100					
Da2				57			
Db1				14			
Db4	6						
Dd1			10				

S3. Fig.s

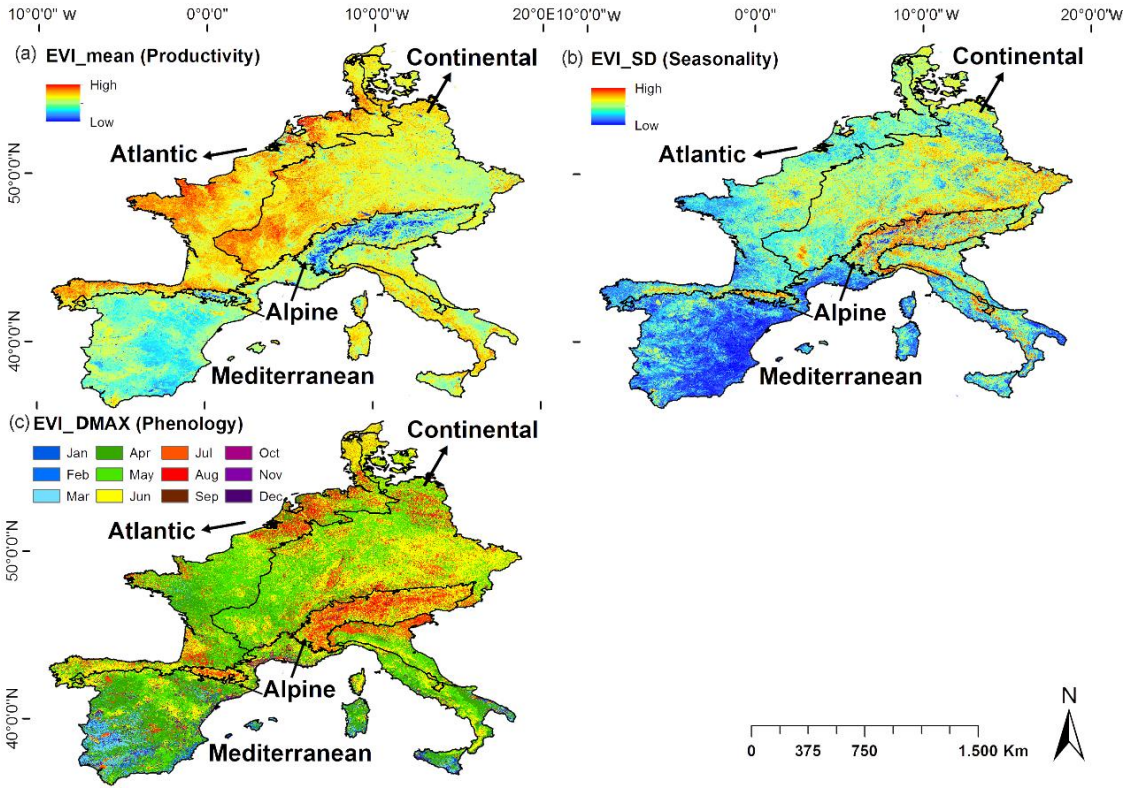

Fig. S1. Ecosystem Functional Attributes based on the 2001-2014 time-series of satellite images of the Enhanced Vegetation Index (EVI) captured by the MODIS-Terra sensor (MOD13Q1.C006 product): (a) EVI annual mean (EVI_mean; an estimator of annual primary production); (b) the EVI seasonal standard deviation (EVI_SD; a descriptor of seasonality); and (c) the date of maximum EVI (EVI_DMAX; an indicator of phenology). Biogeographical regions are based on the official European biogeographical regions map (EEA, 2016).

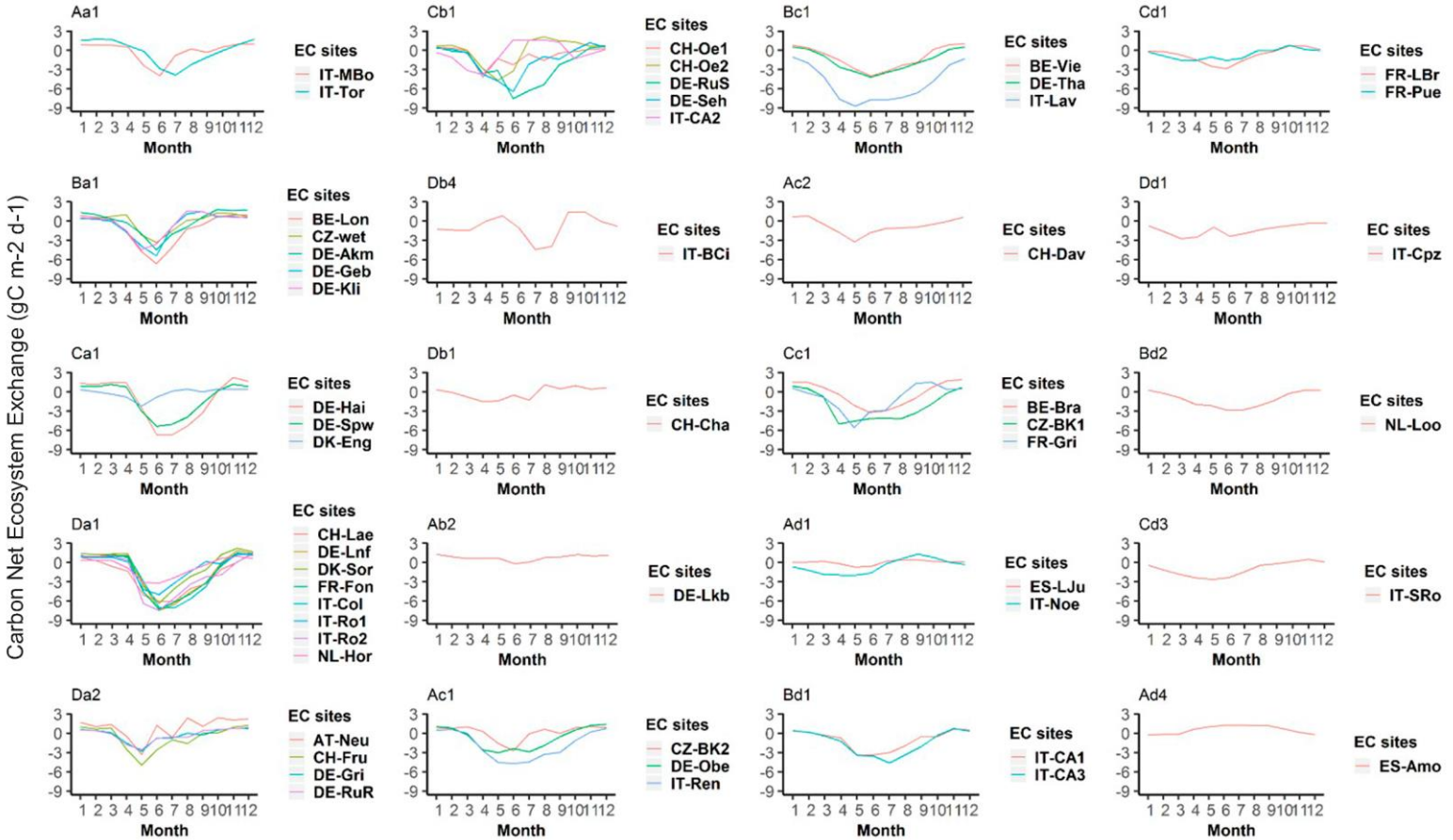

Fig. S2. Variability inter EFTs: annual mean of NEE dynamics from different EC places with the same EFT.

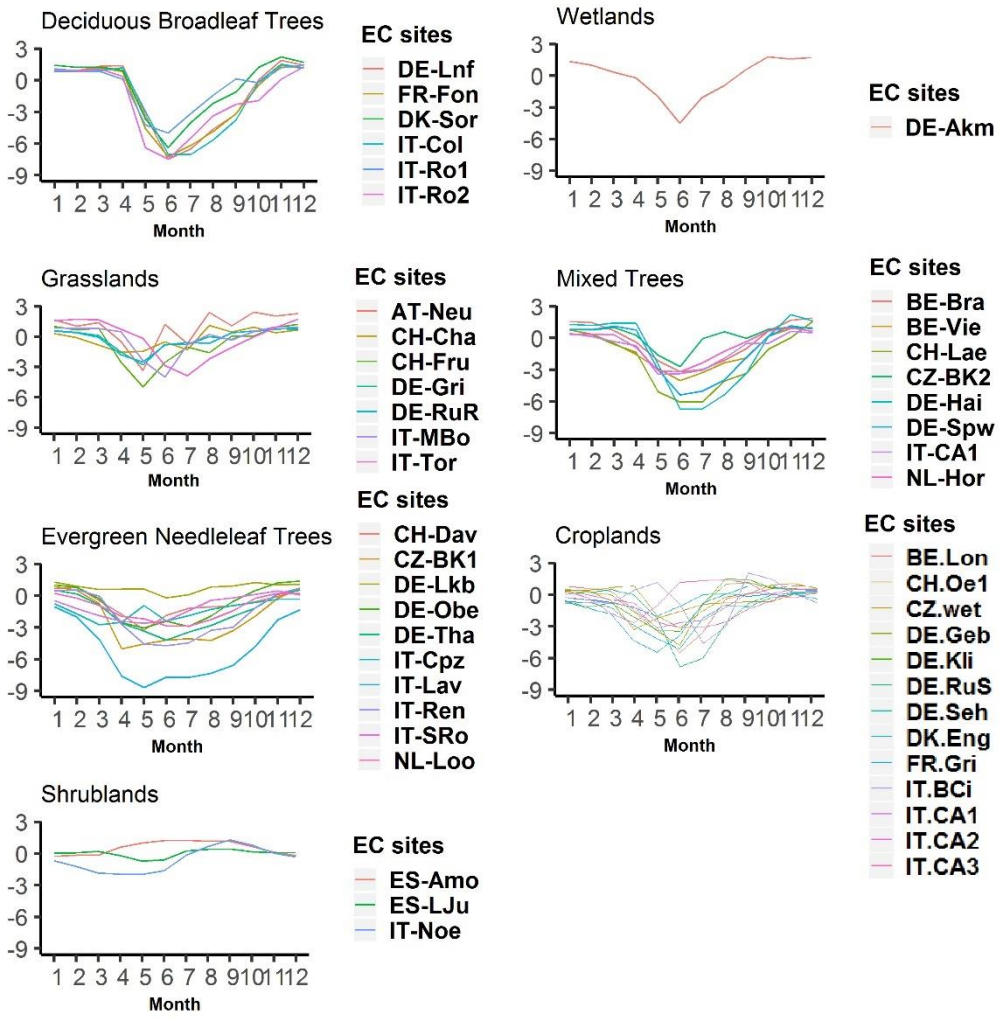

Fig. S3. Variability inter PFTs and intra EFTs: Annual mean of NEE dynamics from different places with the same PFT and different EFT.

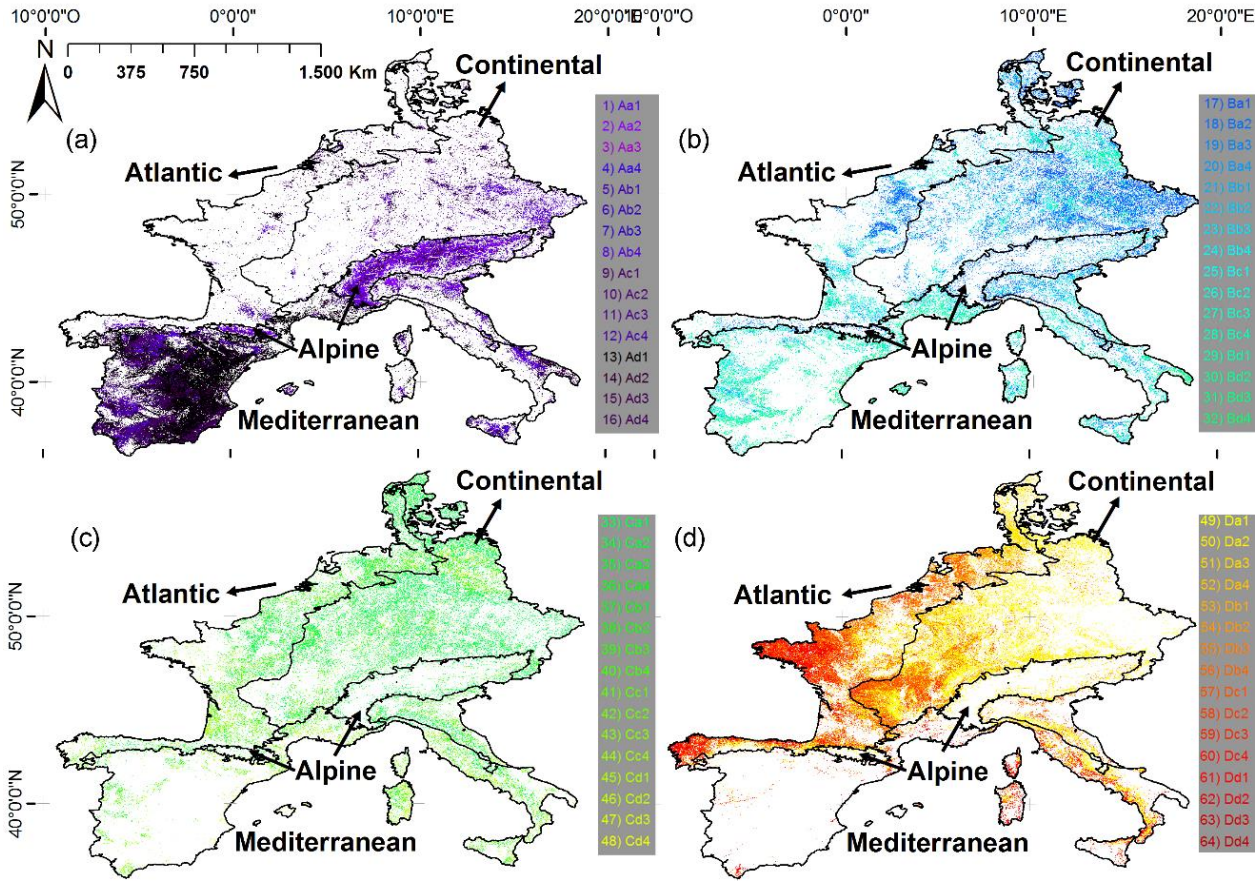

Fig. S4. Ecosystem Functional Types (EFTs) productivity maps based on the 2001-2014 time-series of satellite images of the Enhanced Vegetation Index (EVI) captured by the MODIS-Terra sensor (MOD13Q1.C006 product): (a) EFTs with low productivity (category A) (b) EFTs with low-medium productivity (category B); (c) EFTs with medium-high productivity (category C); and (d) EFTs with high productivity (category D). Biogeographical regions are based on the official European biogeographical regions map (EEA, 2016).

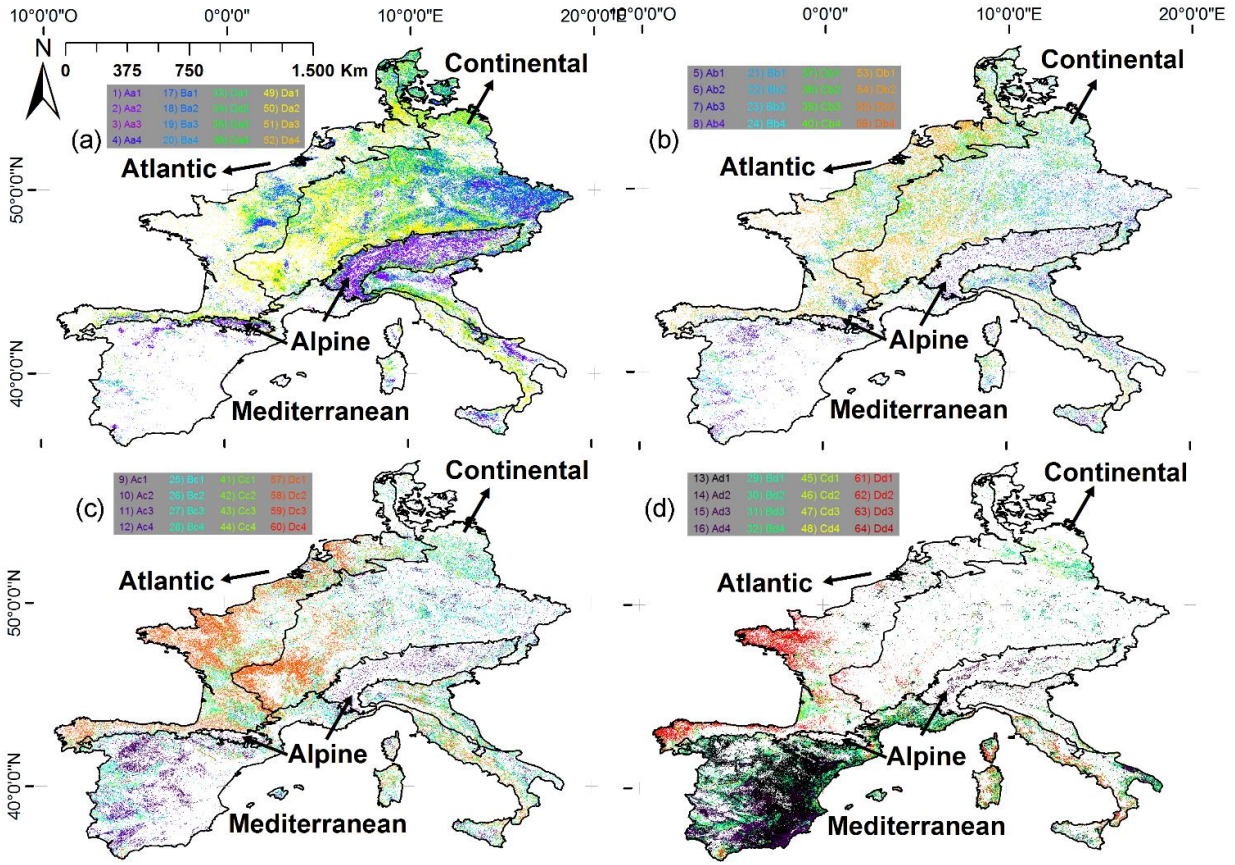

Fig. S5. Ecosystem Functional Types (EFTs) seasonality maps based on the 2001-2014 time-series of satellite images of the Enhanced Vegetation Index (EVI) captured by the MODIS-Terra sensor (MOD13Q1.C006 product): (a) EFTs with high seasonality (category a) (b) EFTs with high-medium seasonality (category b); (c) EFTs with medium-low seasonality (category c); and (d) EFTs with low seasonality (category d). Biogeographical regions are based on the official European biogeographical regions map (EEA, 2016).

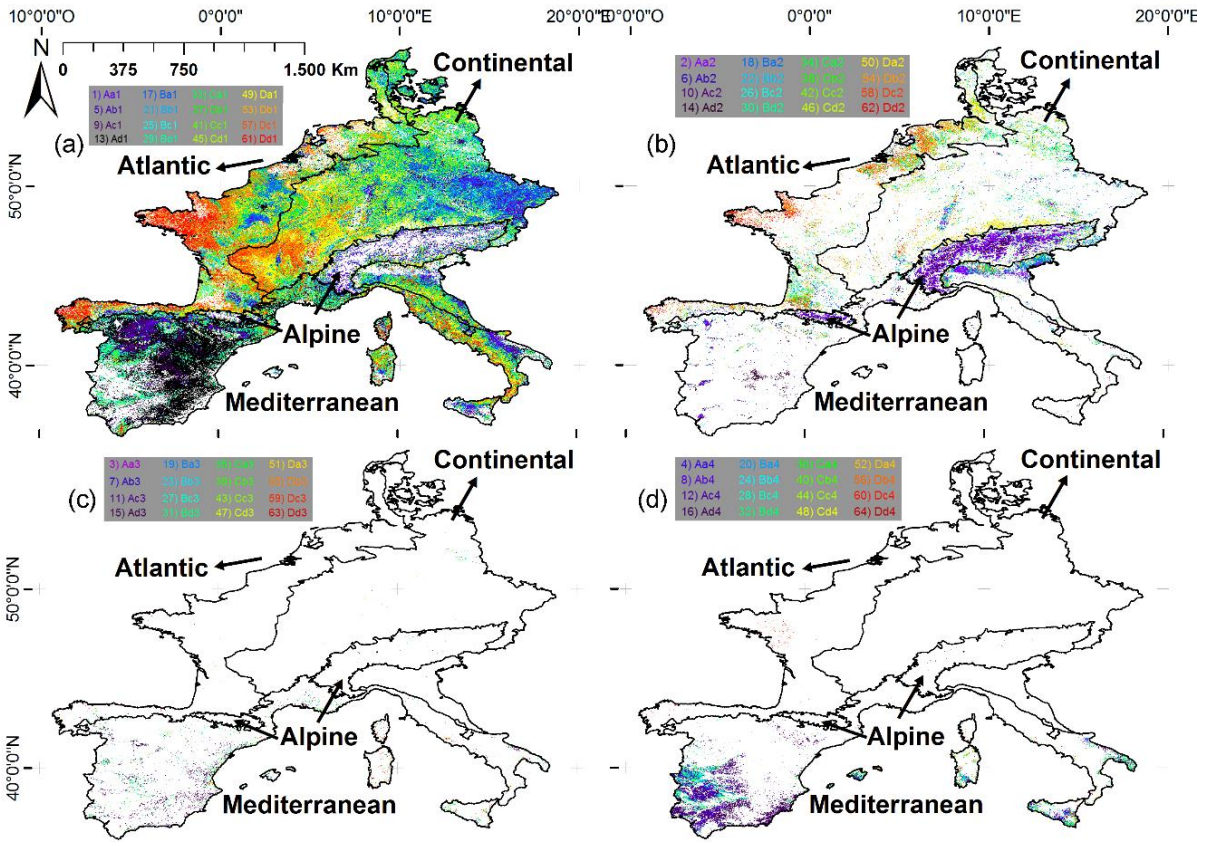
10°0'0"O
0°0'0"
10°0'0"E
20°0'0"E
N
0
375
750
1.500 Km
(a)
(b)
(c)
(d)
Continental
Atlantic
Alpine
Mediterranean
50°0'0"N
40°0'0"N

Fig. S6. Ecosystem Functional Types (EFTs) phenology maps based on the 2001-2014 time-series of satellite images of the Enhanced Vegetation Index (EVI) captured by the MODIS-Terra sensor (MOD13Q1.C006 product): (a) EFTs with spring phenology (category 1) (b) EFTs with summer phenology (category 2); (c) EFTs with autumn (category 3); and (d) EFTs with winter phenology (category 4). Biogeographical regions are based on the official European biogeographical regions map (EEA, 2016).